Continuum diffusion on networks: Trees with hyperbranched trunks and fractal branches

C. P. Haynes and A. P. Roberts
School of Mathematics and Physics, University of Queensland, Queensland 4072, Australia
(Received 9 October 2008; published 18 March 2009)

The probability that a random walker returns to its origin for large times scales as $t^{-\bar{d}/2}$, where $\bar{d}$ is the spectral dimension. We calculate $\bar{d}$ for a class of tree structures using a renormalization technique on an infinite continued fraction. We consider a wide range of homogeneous networks based on replacing the branches of a self-similar tree with arbitrary fractals and composite fractals. We also consider a new class of inhomogeneous hyperbranched trees.

DOI: 10.1103/PhysRevE.79.031111 PACS number(s): 05.40.−a

I. INTRODUCTION

A number of physical [1], chemical [2], and biological [3] problems can be investigated through the study of random walkers on networks. An important parameter of a random walk on an infinite network is the spectral dimension $\bar{d}$ [4], which gives the long time scaling behavior of the probability that a walker returns to its origin $C_0(t) \sim t^{-\bar{d}/2}$. In addition to being an important parameter for characterizing diffusive transport, the spectral dimension is also directly linked to other physical properties of networks [5]. Because of the difficulty of analyzing diffusion on disordered structures, deterministic models, for which exact calculations can be performed, have been studied in great detail [6,7]. The properties of real disordered systems are modeled by studying networks which match measured structural characteristics such as the fractal dimension (d_f) [8], coordination number, and branching and looping behavior. This allows prediction of $\bar{d}$, and hence its dependence on structural factors. In this paper we derive $\bar{d}$ for a wide range of networks by generalizing a class of fractal trees to include hyperbranched trunks and fractal branches.

If a network can be embedded in d dimensional Euclidean space, it is said to be homogeneous and $\bar{d}$ is related to the fractal dimension d_f and the random walk dimension d_w by $\bar{d}=2\frac{d_f}{d_w}$ [6]. For inhomogeneous networks d_f is not defined, and it is not guaranteed that the spectral dimension $\bar{d}$ exists [9]. Finding d_w and $\bar{d}$ for homogeneous networks can be difficult. For finitely ramified deterministic fractals, d_w can be derived using renormalization principles, but for other classes of fractals, d_w often needs to be numerically evaluated through the scaling of the second spatial moment of displacement with time $\langle x^2 \rangle \sim t^{2/d_w}$ [10]. Given the key role that d_w and $\bar{d}$ play in the study of inhomogeneous and homogeneous networks [6,7], their analytic calculation remains a problem of ongoing interest [7,10,11].

For the spectral dimension, there has been significant progress in deriving analytic theorems [12] and exact results for "bundled structures" [13] and "fractal trees" [14–16], structures that are important in physical modeling [13]. Given that a wide variety of fractal structures can occur in nature, it is important to have available as general a class of models as possible. The aforementioned models do not incorporate branches with loops at all scales or hyperbranching, and these features may be important for modeling the properties of polymers [17]. In addition, prior results have been derived for a discrete random walker on structures with branches of integer length. Since certain network problems are more naturally formulated in the continuum (for example, see Refs. [18–20]), it would be useful to derive methods for modeling continuous-time–continuous-space random walkers.

In this paper we present a framework for calculating the spectral dimension of new classes of homogeneous and inhomogeneous structures. The networks incorporate fractal branches, which can contain loops at all scales, as well as hyperbranching in the main trunk. We derive all the results using the continuous-time–continuous-space diffusion equation which allows for noninteger branch lengths. The results can be specialized to discrete-time–discrete-space walkers through simple transformations [21].

In Figs. 1 and 2 we show a schematic of the classes of homogeneous tree fractals we analyze. If the branches of the tree are linear, the structures have been called nice trees of dimension D [14] [Fig. 2(a)]. We derive the spectral dimension for three generalizations of these structures; the case where each branch is a fractal [Fig. 2(b)], where each branch is a composite fractal [Fig. 2(c)] and a third case, where each branch is replaced by an arbitrary finite subnetwork [Fig. 2(d)]. In Fig. 3, we provide an example of the type of inhomogeneous networks that we study in Sec. V.

II. DIFFUSION ON NETWORKS

The probability $C(x,t)$ that a continuous-time–continuous-space random walker is at a point x at time t on a pipe is governed by the diffusion equation

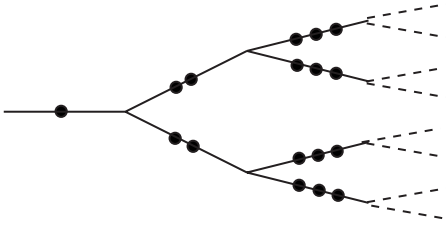

FIG. 1. A Bethe type lattice. We consider networks constructed by replacing the branches of the lattice with a range of different elements. Examples are shown in Fig. 2.

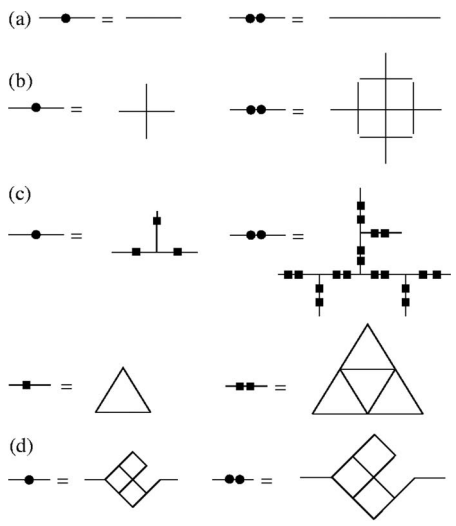

FIG. 2. The types of branches which we can include in the Bethe type network shown in Fig. 1: (a) The standard NT_D tree [14], (b) a fractal branch, (c) a composite fractal branch with loops, and (d) an arbitrary subnetwork.

$$D\frac{\partial^2}{\partial x^2}C(x,t) = \frac{\partial}{\partial t}C(x,t). \tag{1}$$

In order to formulate the equations governing the probability on a network [21], we first solve the diffusion equation on a single pipe for arbitrary Dirichlet conditions and a homogeneous initial condition;

$$C(0,t) = C_0(t), \quad C(b,t) = C_1(t), \quad C(x,0) = 0.$$

Taking Laplace transforms of Eq. (1) and applying the boundary conditions gives

$$c(x,s) = c_1(s)\frac{\sinh(x\sqrt{s/D})}{\sinh(b\sqrt{s/D})} + c_0(s)\frac{\sinh[(b-x)\sqrt{s/D}]}{\sinh(b\sqrt{s/D})},$$

where

$$c(x,s) = \mathcal{L}[C(x,t)] = \int_0^\infty C(x,t)e^{-st}dt.$$

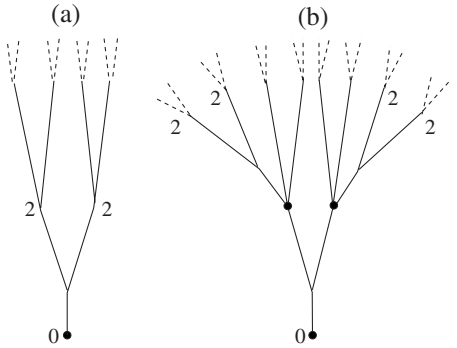

FIG. 3. A nonhomogeneous tree [shown in (b)] created by attaching two copies of the NT_D tree [shown in (a)] to the second row of nodes of a third copy. The spectral dimension of the network created by infinitely extending this idea is given in Sec. V.

The flux entering the pipe at the node $x=0$ is $J_0 = -D\frac{\partial}{\partial x}C(x,t)|_{x=0}$ and the flux entering the pipe at $x=b$ is $J_1 = D\frac{\partial}{\partial x}C(x,t)|_{x=b}$. For networks it is useful to express the fluxes in terms of the concentrations c_i at either end. This gives rise to the equations $\mu\mathbf{j}=E\mathbf{c}$. Here $j_i(s)=\mathcal{L}[J_i(t)]$ are the Laplace transforms of the fluxes, $\mu=\tanh(b\sqrt{\frac{s}{D}})/\sqrt{sD}$ and

$$E = \begin{bmatrix} 1 & -\operatorname{sech}\left(b\sqrt{\frac{s}{D}}\right) \\ -\operatorname{sech}\left(b\sqrt{\frac{s}{D}}\right) & 1 \end{bmatrix}. \tag{2}$$

We call E a flux-concentration matrix and for simplicity we now set D and b to unity. In the remainder of the paper we almost exclusively employ Laplace transformed functions. Rather than explicitly stating this dependence, we henceforth assume this relationship implicitly. Thus "concentration" will refer to the Laplace transform of the concentration, etc.

Using these relations, diffusion on an arbitrary network can be formulated as a system of algebraic equations. To link two or more pipes at a node we set the concentrations to be equal and take the total flux at the node to be zero (mass conservation). The j_i are now taken to represent the total flux entering node i [21]. For mass conservation $j_i=0$, but if we take an instantaneous unit source at node i, then the flux entering the node is $J_i=\delta(t)$ implying that $j_i=\mathcal{L}(J_i)=1$. Examples are shown in Eq. (B1) and Ref. [21].

The inverse of Eq. (2) can be written in the following two useful forms:

$$\begin{bmatrix} c_0 \\ c_1 \end{bmatrix} = \begin{bmatrix} g_{00} & g_{01} \\ g_{10} & g_{11} \end{bmatrix}\begin{bmatrix} j_0 \\ j_1 \end{bmatrix} = g_{00}\begin{bmatrix} 1 & f \\ f & 1 \end{bmatrix}\begin{bmatrix} j_0 \\ j_1 \end{bmatrix}. \tag{3}$$

Here g_{ij} are Green's functions and $f=g_{01}/g_{00}$ is a first passage time. Their precise definitions are provided in Appendix A. In the second form we have used the fact that $g_{11}=g_{00}$ and $g_{01}=g_{10}$. While this is obvious for a single pipe, it actually holds for any symmetric network (see Sec. VI). Of course g_{ij} and f are actually the Laplace transforms of their underlying functions.

The second form provided in Eq. (3) can also be written as

$$g_{00}(1-f^2)\begin{bmatrix} j_0 \\ j_1 \end{bmatrix} = \begin{bmatrix} 1 & -f \\ -f & 1 \end{bmatrix}\begin{bmatrix} c_0 \\ c_1 \end{bmatrix}, \tag{4}$$

which allows a direct comparison with Eq. (2). This shows that $\operatorname{sech}(\sqrt{s})$ is a first passage time and $\mu=g_{00}(1-f^2)$. Both forms of the flux-concentration equations (3) and (4) are employed throughout the paper.

A. Two illustrative examples

Consider connecting three pipes of different lengths end to end. The system of equations for the pipes $(i=0,1,2)$ is

$$\begin{bmatrix} c_0^{(i)} \\ c_1^{(i)} \end{bmatrix} = g_{00}^{(i)}\begin{bmatrix} 1 & f^{(i)} \\ f^{(i)} & 1 \end{bmatrix}\begin{bmatrix} j_0^{(i)} \\ j_1^{(i)} \end{bmatrix}, \tag{5}$$

where $g_{00}^{(i)}$ and $f^{(i)}$ are the respective functions for the ith pipe. If we attach the right end node of the zeroth pipe to the

left end node of the first pipe we must have $j_1^{(0)}+j_0^{(1)}=0$ and $c_0^{(1)}=c_1^{(0)}$. At the junction of the first and second pipe we have $j_1^{(1)}+j_0^{(2)}=0$ and $c_0^{(2)}=c_1^{(1)}$.

For our example, taking the boundary conditions $j_0^{(0)}=1$ and $j_1^{(2)}=0$ corresponds to the case of a walker released at the left end node of pipe 0 and a reflective boundary condition at the right end node of pipe 2. Note that there are six equations: two boundary conditions, two continuity, and two mass conservation conditions. These fully determine the six unknown fluxes and concentrations within the system. In particular, we are interested in finding $C_0(t)$ $[c_0(s)]$ which we obtain through an iterative procedure.

Taking $j_1^{(2)}=0$ for the second pipe gives $j_0^{(2)}=c_0^{(2)}/g_{00}^{(2)}$. We write this relationship as $j_0^{(2)}=h_2c_0^{(2)}$, with $h_2=1/g_{00}^{(2)}$. We now set $j_1^{(1)}=-h_2c_1^{(1)}$, where we have used the fact that $j_1^{(1)}+j_0^{(2)}=0$ and $c_0^{(2)}=c_1^{(1)}$. This leads to the system of equations

$$\begin{bmatrix} c_0^{(1)} \\ c_1^{(1)} \end{bmatrix} = g_{00}^{(1)} \begin{bmatrix} 1 & f^{(1)} \\ f^{(1)} & 1 \end{bmatrix} \begin{bmatrix} j_0^{(1)} \\ -h_2c_1^{(1)} \end{bmatrix}. \tag{6}$$

Using the second of these equations, we can express $c_1^{(1)}$ in terms of $j_0^{(1)}$ to give $c_1^{(1)}=(1+g_{00}^{(1)}h_2)^{-1}g_{00}^{(1)}f^{(1)}j_0^{(1)}$. Substituting $c_1^{(1)}$ into the first row of Eq. (6) gives

$$c_0^{(1)} = g_{00}^{(1)}[1 - g_{00}^{(1)}(f^{(1)})^2h_2(1 + g_{00}^{(1)}h_2)^{-1}]j_0^{(1)}.$$

This equation can be expressed as $j_0^{(1)}=h_1c_0^{(1)}$, where h_1 depends on h_2 but not on $c^{(i)}$ or $j^{(i)}$ $(i=1,2)$. In a similar way, we can write $j_0^{(0)}=h_0c_0^{(0)}$, where h_0 depends only on h_1. To determine $c_0^{(0)}$, we apply the boundary condition $j_0^{(0)}=1$ which gives $c_0^{(0)}=(h_0)^{-1}$. The remaining variables $c_1^{(i)}$ and $j_1^{(i)}$ (for $i\geqslant 1$) can be found by backward substitution. Here, our goal is to find $c_0^{(0)}$, so $c_1^{(i)}$ and $j_1^{(i)}$ for $i\geqslant 1$ do not need to be explicitly determined.

As a second example, we consider attaching two identical pipes, "1" and "1a," to the end of pipe "0." The equations for the three pipes are identical to Eq. (5) with labels $i=0,1,1a$. By analogy with the previous problem, we have the continuity conditions $c_1^{(0)}=c_0^{(1)}=c_0^{(1a)}$, the mass conservation condition $j_0^{(1)}+j_0^{(1a)}+j_1^{(0)}=0$, and we take the boundary conditions to be $j_0^{(0)}=1$ and $j_1^{(1a)}=j_1^{(1)}=0$. If we set $j_0^{(1a)}=h_{1a}c_0^{(1a)}$ and $j_0^{(1)}=h_1c_0^{(1)}$, we can reduce the problem to the two by two system,

$$\begin{bmatrix} c_0^{(0)} \\ c_1^{(0)} \end{bmatrix} = g_{00}^{(0)} \begin{bmatrix} 1 & f^{(0)} \\ f^{(0)} & 1 \end{bmatrix} \begin{bmatrix} j_0^{(0)} \\ -(h_1+h_{1a})c_1^{(0)} \end{bmatrix}.$$

Since pipe 1 and 1a are identical, $h_1=h_{1a}$, allowing us to write $j_1^{(0)}=-uh_1c_1^{(0)}$ where u is the number of identical pipes attached at the right end node of network 0 ($u=2$ above). To determine $c_0^{(0)}$, the solution procedure is essentially identical to that used in the first example.

B. Connection of n pipes

We now consider an arbitrary number of elements where the pipes of the nth generation are denoted by ℓ_n. To analyze Bethe type networks, we form the $(n+1)$th generation by connecting u pipes to each pipe ℓ_n at the node $n+1$, as described in the second example given in Sec. II A. The case $u=2$ is shown in Fig. 1. We no longer need to label or explicitly consider the side branches; node n and pipe n will refer to the obvious locations in the main branch. We distinguish local and global quantities as follows; $g_{00}^{(n)}$ and $f^{(n)}$ are the functions g_{00} and f, respectively, for the nth pipe. Likewise $j_0^{(n)}$ is the flux at node 0 of the nth pipe. If no superscript is used, then the quantity corresponds to the entire network, i.e., c_n refers to the concentration at node n of the entire network.

Using this new notation, Eq. (5) for the nth pipe is

$$g_{00}^{(n)} \begin{bmatrix} 1 & f^{(n)} \\ f^{(n)} & 1 \end{bmatrix} \begin{bmatrix} j_0^{(n)} \\ j_1^{(n)} \end{bmatrix} = \begin{bmatrix} c_n \\ c_{n+1} \end{bmatrix}. \tag{7}$$

Observe, from the examples provided in Sec. II A, that we can set $j_1^{(n)}=-uh_{n+1}c_{n+1}$ and $j_0^{(n)}=h_nc_n$. It was implicitly proved that $j_0^{(n)}=h_nc_n$ for any terminating network and hence, following the argument in Sec. II A, the mass conservation condition implies $j_1^{(n)}=-uh_{n+1}c_{n+1}$. This transformation appears to allow $c_n=c_{n+1}=0$ as a solution to Eq. (7). We ignore this unphysical case and require $c_n>0$ and $c_{n+1}>0$. The equations are then solved to determine h_n in terms of h_{n+1} to give

$$(g_{00}^{(n)}h_n)^{-1} = 1 - (f^{(n)})^2[1 + (g_{00}^{(n)}uh_{n+1})^{-1}]^{-1}. \tag{8}$$

For reasons that will become clear in the next section, we rewrite Eq. (8) by multiplying the term $(g_{00}^{(n)}uh_{n+1})^{-1}$ in the right-hand side (RHS) of Eq. (8) by $g_{00}^{(n+1)}/g_{00}^{(n+1)}$;

$$(g_{00}^{(n)}h_n)^{-1} = 1 - (f^{(n)})^2\left(1 + \frac{g_{00}^{(n+1)}}{ug_{00}^{(n)}}(g_{00}^{(n+1)}h_{n+1})^{-1}\right)^{-1}. \tag{9}$$

Either of Eqs. (8) or (9) allow all the h_i to be determined for a finite network. The no-flux boundary condition is incorporated by taking $h_{n+1}=0$, where $n+1$ is the final node of the network. c_0 can then be found from $c_0=1/h_0$. The functions $1/h_n$ are the return to origin Green's functions for the network that lies to the right of node n.

For a discrete random walker, it is well known that the probability generating functions associated with random walk quantities on tree lattices can be expressed in terms of a continued fraction [22]. To our knowledge, this is the first time the infinite continued fraction for a continuous time–continuous space random walker has been formulated.

III. PRIOR RESULTS

It is useful to show how the continued fraction can be used to derive earlier results. The ideas will be used in subsequent sections. We first find c_0 for the infinite Bethe lattice [23,24] with co-ordination number $u+1$. The relevant system for the problem is

$$\frac{\coth(\sqrt{s})}{\sqrt{s}} \begin{bmatrix} 1 & \operatorname{sech}(\sqrt{s}) \\ \operatorname{sech}(\sqrt{s}) & 1 \end{bmatrix} \begin{bmatrix} j_0^{(n)} \\ j_1^{(n)} \end{bmatrix} = \begin{bmatrix} c_n \\ c_{n+1} \end{bmatrix}. \tag{10}$$

For simplicity, we have used explicit expressions for $g_{00}^{(n)}$ and $f^{(n)}$. A recurrence relationship is obtained by taking $j_1^{(n)}=-uh_{n+1}c_{n+1}$ and $j_0^{(n)}=h_nc_n$ in Eq. (10) and solving for h_n to get

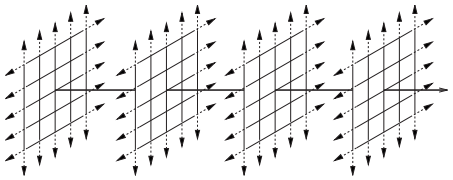

FIG. 4. The continued fraction method can be used to rederive a result for the kebab lattice [25].

$$h_n = \sqrt{s}\left(\coth(\sqrt{s}) - \frac{\operatorname{csch}(\sqrt{s})^2\sqrt{s}}{uh_{n+1} + \sqrt{s}\coth(\sqrt{s})}\right). \tag{11}$$

If we consider infinitely many pipes ($n \to \infty$), then the continued fraction given in Eq. (11) becomes an infinite periodic fraction. Replacing h_n and h_{n+1} by h_0 and solving the resultant quadratic gives

$$c_0 = \frac{1}{h_0} = \frac{2u\tanh(\sqrt{s})s^{-1/2}}{(u-1) + \sqrt{(u-1)^2 + 4u\tanh(\sqrt{s})^2}}.$$

c_0 must be multiplied by $u+1$ to model a full Bethe lattice as we have only considered one of $u+1$ branches. The expression is equivalent to prior results [23,24] if the continuum-discrete transformation [21] is applied.

We now consider classes of networks obtained by adding a branch at every node $i \geqslant 1$ of the basic Bethe lattice. The attachment of a branch B implies the total flux entering the nth pipe at node $n+1$ is now the addition of two fluxes; the flux from the $(n+1)$th pipe and the flux from the branch. We therefore take $j_1^{(n)} = -uh_{n+1}c_{n+1} - h_n^B c_{n+1}$ and $j_0^{(n)} = h_n c_n$ in Eq. (7) to derive a recurrence relationship for the modified network:

$$(g_{00}^{(n)}h_n)^{-1} = 1 - (f^{(n)})^2 \times \{1 + [g_{00}^{(n)}(uh_{n+1} + h_n^B)]^{-1}\}^{-1}. \tag{12}$$

Here, h_n^B is associated with the branch attached to the nth node of the network.

Consider an infinite pipe ($u=1$) composed of finite pipes n having identical lengths with an identical branch B ($h_n^B = h^B$) attached at every node. In this case, the recurrence relationship (12) reduces to

$$h_n = \sqrt{s}\left(\coth(\sqrt{s}) - \frac{\operatorname{csch}(\sqrt{s})^2\sqrt{s}}{h_{n+1} + h^B + \sqrt{s}\coth(\sqrt{s})}\right),$$

which can be solved, since it is a periodic infinite fraction, to give

$$h_0 = \frac{1}{2}(-h^B + \sqrt{(h^B)^2 + 4\sqrt{s}\coth(\sqrt{s})h^B + 4s}). \tag{13}$$

As an example, the function h^B for a two-dimensional (2D) lattice can be found [21] from its discrete counterpart [26] giving $h^B = \tanh(\sqrt{s})K[\operatorname{sech}(\sqrt{s})^2]/(2\pi\sqrt{s})$, where $K(x)$ is the complete Elliptic integral of the first kind [27]. Using this in Eq. (13), gives c_0 for a semi-infinite kebab lattice as shown in Fig. 4 [25]. Likewise c_0 for a semi-infinite 2D comb lattice is taken by attaching two infinite pipes at every node, implying that $h^B = 2\sqrt{s}$. One can construct c_0 for a d-dimensional comb [28] through similar arguments. All of these examples are cases of bundled structures whose spectral dimensions were derived in [13].

IV. SPECTRAL DIMENSION OF NT_D TREES

Although Eq. (9) provides a formal solution for h_0, the analysis of the infinite continued fraction is greatly simplified if the pipes of generation ℓ_n scale in a particular way. In this section we focus on the nth pipe having length 2^{vn}, where $v > 0$. For the examples in the previous section $v=0$. For $v>0$ and integer, the resultant networks have been called NT_D trees [15]. Here we show how to renormalize the continued fraction to obtain the spectral dimension for these networks.

Since every pipe has length 2^{vn}, $f^{(n)} = \operatorname{sech}(2^{vn}\sqrt{s})$ and $g_{00}^{(n)} = \coth(2^{vn}\sqrt{s})/\sqrt{s}$ [this follows from Eqs. (2) and (3)]. Note that $f^{(n)}$ and $g_{00}^{(n)}$ have the following key properties:

$$f^{(n)}(\rho(s)) = f^{(n+1)}(s), \tag{14}$$

$$\frac{g_{00}^{(n+1)}(\rho(s))}{g_{00}^{(n)}(\rho(s))} = \frac{g_{00}^{(n+2)}(s)}{g_{00}^{(n+1)}(s)}, \tag{15}$$

where $\rho(s) = 4^v s$. The function $\rho(s)$ is introduced to allow the results to be extended to more general fractals later.

Now because $g_{00}^{(n)}h_n$ given in Eq. (9) is a function of $f^{(n)}$, $g_{00}^{(n+1)}/g_{00}^{(n)}$ and $g_{00}^{(n+1)}h_{n+1}$, we can exploit the properties of Eqs. (14) and (15) to relate $g_{00}^{(n)}h_n$ to $g_{00}^{(n+1)}h_{n+1}$. In doing so, it can be shown that it is possible to transform the infinite continued fraction (9) for h_0 to a finite continued fraction.

Setting $s = \rho(s)$ in the RHS of Eq. (9) and using Eqs. (14) and (15) returns the RHS of Eq. (9) with n replaced by $n+1$ which is just $(g_{00}^{(n+1)}h_{n+1})^{-1}$. Therefore for an infinite network

$$[g_{00}^{(n)}(\rho)h_n(\rho)]^{-1} = (g_{00}^{(n+1)}h_{n+1})^{-1}. \tag{16}$$

For a finite network the continued fraction terminates and this equation does not hold.

When $n=0$, we find that

$$\frac{g_{00}^{(1)}}{g_{00}^{(0)}(\rho)h_0(\rho)} = h_1^{-1}. \tag{17}$$

This equation provides a second relationship between h_0 and h_1 which can be combined with the first step of the iterative process given in Eq. (9) to eliminate h_1 and express h_0 in terms of $h_0(\rho)$.

From Eq. (9) we know that h_0 is given by

$$(g_{00}^{(0)}h_0)^{-1} = 1 - (f^{(0)})^2[1 + (g_{00}^{(0)}uh_1)^{-1}]^{-1}. \tag{18}$$

Substituting Eq. (17) into Eq. (18) gives

$$(g_{00}^{(0)}h_0)^{-1} = 1 - (f^{(0)})^2\left(1 + \frac{g_{00}^{(1)}(h_0(\rho))^{-1}}{g_{00}^{(0)}ug_{00}^{(0)}(\rho)}\right)^{-1}.$$

This equation represents a renormalization of the infinite continued fraction for h_0, and is the key to the results of this paper.

To finally relate the problem to c_0, we recall that $c_0 = 1/h_0$ and $g_{00}^{(0)} f^{(0)} = g_{ij}^{(0)}$, which gives an implicit equation for c_0:

$$c_0 = g_{00}^{(0)} - (g_{01}^{(0)})^2 \left(g_{00}^{(0)} + \frac{g_{00}^{(1)} c_0(\rho)}{u g_{00}^{(0)}(\rho)} \right)^{-1}. \tag{19}$$

A. Asymptotic analysis

From the expression (19) for $c_0(s)$, we can find the long time asymptotic behavior of $C_0(t)$ by analyzing $c_0(s)$ as $s \to 0$. If $C_0(t) \sim t^{-\delta-1}$ as $t \to \infty$ then, by standard Tauberian theorems [29,30], it can be shown that $c_0(s)$ has the following behavior as $s \to 0$:

$$c_0 = \begin{cases} k_1 s^{\delta} + O(s^{\delta+1}) & -1 < \delta < 0 \\ k_0 s^{\delta} \ln(s) + O(s^{\delta+1} \ln(s)) & \delta = 0,1,2,\ldots \\ k_0 + k_1 s^{\delta} + O(s^{\delta+1}) & \delta > 0,\ \delta \neq 0,1,\ldots \end{cases}, \tag{20}$$

where k_i are constants. Since $g_{ij}^{(n)}(s)$ are Green's functions of finite structures, they must have the following series expansion:

$$g_{ij}^{(n)}(s) = (sA_n)^{-1} + O(s^0), \tag{21}$$

where A_n is the mass of ℓ_n. This is a direct consequence of the fact that as $t \to \infty$, the probability of being at the origin (or indeed any node) of the finite pipe is equal to the reciprocal of the mass of the pipe. Although length and mass are identical for a pipe, for the more general elements considered in later sections, the mass and length differ.

Using the asymptotic forms (20) and (21) in Eq. (19) and equating coefficients of the resultant expansion, we find that

$$1 = \frac{4^{v\delta+v}}{uA},$$

for all possible cases of δ, implying that $\delta = -1 + \ln(Au)/\ln(4^v)$. In the above, $A = 2^v$ denotes the fractional increase in the length of the pipe for each iteration.

Finally, in order to calculate the spectral dimension, it is clear that $\delta = \bar{d}/2 - 1$. Hence

$$\bar{d} = 1 + 2\frac{\ln(u)}{v \ln(4)}, \tag{22}$$

which agrees with prior results [31] if v is an integer. For the continuum case v can be any positive number. Given that the calculation of the spectral dimension is not dependent on the chosen starting site within the infinite network [32], we only need to perform the asymptotic analysis at one node. In subsequent sections we apply the renormalization and scaling ideas to new classes of networks.

V. INHOMOGENEOUS NETWORKS

We now calculate $\bar{d}$ for an interesting class of inhomogeneous networks generated iteratively. Let β_0 denote an infinite network with origin at node 0 and spectral dimension $\bar{d}_0$. Now attach the origin of β_0 to node i of a copy of β_0, and denote the new network as β_1 (the origin of β_1 is the same as the origin of β_0). Next, attach the origin of β_1 to node i of a new copy of β_0 to form β_2 and so on. The resultant infinite network β_∞ has no fractal dimension (i.e., it is inhomogeneous). As an elementary example, let β_0 be an infinite pipe and set $i=1$, in which case β_∞ is a comb with infinite branches.

As in previous sections, our aim is to calculate $c_0 = 1/h_0$. The sequence h_n is given by Eq. (8) with the exception of h_{i-1} which is equal to

$$(g_{00}^{(i-1)} h_{i-1})^{-1} = 1 - (f^{(i-1)})^2 \times \{1 + [g_{00}^{(i-1)}(uh_i + h_i^B)]^{-1}\}^{-1}. \tag{23}$$

The function $1/h_i^B$ is the Green's function of the added network B. This network is equivalent to β_∞ except that it has one branch (β_0) removed. The two structures are essentially equivalent, and therefore must share the same Green's function, so $1/h_i^B = 1/h_0$. The function $1/h_i$ in Eq. (23) is the Green's function of the remainder of the original network. Because it is just a rescaled version of β_0, its scaling behavior is identical to that of β_0 which can be obtained from Eq. (20) with $\delta = \bar{d}_0/2 - 1$. Equation (23) now gives h_{i-1} in terms of a function of known scaling h_i and the function $h_i^B(=h_0)$ which at this stage is unknown, but it is to be determined.

We now eliminate $h_1, h_2, \ldots, h_{i-2}$ from Eq. (8) to express h_0 as a function of h_{i-1}, and hence as a function of h_i and $h_i^B(=h_0)$. It is clear that h_0 is a function of h_1, and h_1 is a function of h_2, etc. We can eliminate all intermediate h_n ($1 \leqslant n < i-1$) by repeated substitution in the continued fraction to obtain a result of the form

$$h_0 = \frac{1}{\alpha_1} \frac{\alpha_3 h_{i-1} + 1}{\alpha_2 h_{i-1} + 1}, \tag{24}$$

where α_i are functions of s. Using the fact that $c_0 = 1/h_0$ we have

$$c_0 = \alpha_1 \frac{\alpha_2 h_{i-1} + 1}{\alpha_3 h_{i-1} + 1}. \tag{25}$$

To derive the scaling behavior of each α_i we consider three problems on finite networks associated with β_0. First, consider the truncated network "I" created by terminating the network at node $i-1$ with a zero flux boundary condition ($h_{i-1}^I = 0$). With $h_{i-1}^I = 0$, Eq. (25) becomes $c_0^I = \alpha_1(s)$, which is now the Green's function for the finite network I with total mass M_{i-1}. Thus $\alpha_1 = 1/(M_{i-1}s) + O(s^0)$.

We now take a homogeneous Dirichlet condition at node $i-1$ of network I ($c_{i-1}^{I*} = 0$). This is equivalent to taking $h_{i-1}^{I*} \to \infty$, in which case Eq. (25) becomes $c_0^{I*} = \alpha_1 \alpha_2 / \alpha_3$, where c_0^{I*} is the concentration at the origin of the modified problem. Since $C_0^{I*}(t) \to 0$ as $t \to \infty$, $c_0^{I*}(s) = \mathcal{L}[C_0^{I*}(t)]$ is nonsingular at $s=0$, and therefore $c_0^{I*} = O(s^0)$.

Finally, consider the truncated network II formed by terminating the network at node i with a zero flux boundary condition ($h_i^{II} = 0$). If we set $h_i^{II} = 0$ in Eq. (8) then $h_{i-1}^{II} = 1/g_{00}^{(i-1)}$. Rewriting Eq. (25) for network II gives

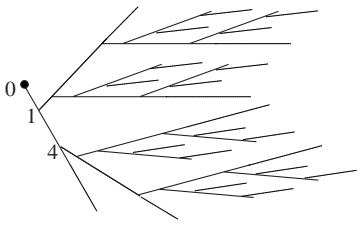

FIG. 5. An inhomogeneous tree created from an infinite pipe with two iterative attachment points located at nodes $i_1=1$ and $i_2=4$.

$$c_0^{II} = \alpha_1(s)\frac{\alpha_2(s)/g_{00}^{(i-1)}+1}{\alpha_3(s)/g_{00}^{(i-1)}+1},$$

where we denote the concentration at the origin as c_0^{II}. This must scale as $c_0^{II}=1/(M_i s)+O(s^0)$, where $M_i=M_{i-1}+uA_{i-1}$ is the mass of the finite network *II*. Using $g_{00}^{(i-1)}=1/(A_{i-1}s)+O(s^0)$ and the asymptotic forms of $\alpha_1(s)$, $\alpha_2(s)$ and c_0^{II} it can be shown that $\alpha_3=u/(sM_{i-1})+O(s^0)$.

Substituting h_{i-1} from Eq. (23) into Eq. (24) gives a quadratic equation in terms of h_0 where the scaling of all the other terms are known. We can now find the scaling of h_0 and hence c_0. Note the above only holds for $i\geqslant 2$. If $i=1$ then Eq. (23) is directly a quadratic in h_0 and the scaling of h_1 follows that of h_0 of the base network β_0. If the base homogeneous network β_0 has spectral dimension $\bar{d}_0$, the spectral dimension for β_∞ can be shown to be

$$\bar{d} = \begin{cases} 4-\bar{d}_0 & \bar{d}_0<2,\ u\geqslant 2 \text{ and } i\neq 1 \\ 1+\bar{d}_0/2 & \bar{d}_0<2,\ [u=1 \text{ or } i=1] \\ \bar{d} & \bar{d}_0>2 \end{cases}$$

The networks with $\bar{d}=1+\bar{d}_0/2$ are comb type networks. For example, if $u=1$, then β_0 is a pipe with $\bar{d}_0=1$ and β_∞ is a comb with $\bar{d}=3/2$. The answer is identical to that obtained if Eq. (13) is solved with $h_B=\sqrt{s}$. If $i=1$ and β_0 is say, an NT_D tree (see Sec. IV), then β_∞ has a spectral dimension $\bar{d}=1+\bar{d}_0/2$ if $\bar{d}_0<2$ or $\bar{d}=\bar{d}_0$ if $\bar{d}_0>2$. These networks can be thought of as bundled structures [13].

If the attachment node $i\geqslant 2$ then the resultant nonhomogeneous networks are neither combs or bundled structures. As an example, if β_0 is an NT_D tree with $i=2$ and $u=2$ then we obtain a network shown in Fig. 3. In this section we have only considered generating iterative structures through the node i, however, a multitude of new networks are possible if two (or more) nodes are used. In Fig. 5, we show an example of a pipe with $i_1=1$ and $i_2=4$. The equation for h_0 becomes a cubic and scaling arguments show that $\bar{d}=3$.

VI. FRACTAL BRANCHES

Until now the elements ℓ_n have been pipes of length 2^{vn}. We now model structures where each pipe ℓ_n is replaced by the (vn)th iteration of a finitely ramified deterministic symmetric fractal $\mathcal{F}$ (where v is now integer). An example is shown in Fig. 6. Here we show that the results of the previous sections can be simply modified for this case.

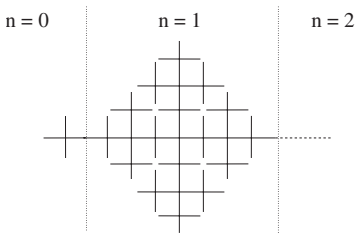

FIG. 6. A deterministic fractal tree with $v=2$, $u=1$.

Consider a flux-concentration matrix for a fractal with N nodes of the form $\mu\mathbf{j}=E\mathbf{c}$, with $\mathbf{j}^T=(j_0,0,\ldots,0,j_1)$. If we ignore the first and last equations we have an underdetermined system of $N-2$ equations for N variables. This can be rearranged to express the $N-2$ intermediate concentrations in terms of c_0 and c_1 (see Appendix B and [21] for an example). After substitution, we find the $N\times N$ equations are replaced by the 2×2 system:

$$\mu\begin{bmatrix} j_0 \\ j_1 \end{bmatrix} = \begin{bmatrix} \bar{E}_{00} & \bar{E}_{01} \\ \bar{E}_{10} & \bar{E}_{11} \end{bmatrix}\begin{bmatrix} c_0 \\ c_1 \end{bmatrix}. \tag{26}$$

The reduction of E to a 2×2 matrix $\bar{E}$ can be performed for arbitrary networks with two exterior connections. $\bar{E}$ is the flux-concentration matrix for an "effective reduced network."

Re-writing the equations for the effective reduced networks as in Eq. (3) for iteration n gives

$$\begin{bmatrix} c_n \\ c_{n+1} \end{bmatrix} = g_{00}^{(n)}\begin{bmatrix} 1 & f^{(n)} \\ f^{(n)} & 1 \end{bmatrix}\begin{bmatrix} j_0^{(n)} \\ j_1^{(n)} \end{bmatrix}, \tag{27}$$

where $g_{00}^{(n)}$ and $f^{(n)}$ are Green's functions and first passage times associated with the fractal ℓ_n. Writing the matrix in the form shown in Eq. (27) requires $g_{11}=g_{00}$ and $g_{01}=g_{10}$. This restricts our results to fractals with end-to-end symmetry.

Since these equations have an identical form to Eq. (7) all of the results in Sec. IV can be extended if Eqs. (14) and (15) hold. Since $f^{(n)}$ is a first passage time of a finitely ramified deterministic fractal, there exists a $\rho(s)$ such that $f^{(n)}(s)=f^{(n-1)}(\rho(s))$ [33,34]. An example is given in Appendix B. The second Eq. (15) also holds for any $\mathcal{F}$ (see Appendix C).

In order to apply the series expansions provided in Sec. IV A, we note that $\rho(s)$ has the following Taylor series expansion:

$$\rho(s) = a^v s + O(s^2),$$

where a is linked to the random walk dimension d_w of $\mathcal{F}$ such that $a=L^{d_w}$. Here L is the rescaling of length from the ith to the $(i+1)$th iteration of $\mathcal{F}$. The Sierpinski gasket, for example, has $L=2$, $d_w=\ln(5)/\ln(2)$ and $a=5$. The pipe used in the NT_D (Sec. IV) tree can be viewed as a fractal with $L=2$ and $d_w=2$ which implies that $a=2^2=4$. For the pipe, note that $\rho(s)=4^v s$ exactly. The appearance of the exponent v for $v\geqslant 2$ in the expansion of $\rho(s)$ is explained in Appendix B.

The analysis presented in Sec. IV A holds for arbitrary $\rho(s)$ and gives

$$\bar{d} = 2\frac{\ln(u)}{v\ln(a)} + \bar{d}_{\mathcal{F}}.$$

Here $\bar{d}_{\mathcal{F}}$ is the spectral dimension of $\mathcal{F}$ used to construct the network. If the fractal is a pipe then $\bar{d}_{\mathcal{F}}=1$ and the result agrees with Eq. (22).

VII. COMPOSITE FRACTAL BRANCHES

We now consider fractal subnetworks $\ell_0, \ell_1, \ldots, \ell_n$, where the pipes of each fractal are themselves replaced by another fractal. We take the subnetwork ℓ_n to be a fractal $\mathcal{F}(1)$ of iteration $v(1)n$. We now replace all of the pipes in the subnetwork by a fractal $\mathcal{F}(2)$ of iteration $v(2)n$. An example is given in Fig. 2(c): $\mathcal{F}(1)$ is a T tree of iteration n (i.e., $v(1)=1$) and $\mathcal{F}(2)$ is a Sierpinski gasket of iteration $n[v(2)=1]$.

For the nth iteration the inverse flux-concentration equations of the effective reduced network are

$$\begin{bmatrix} c_n \\ c_{n+1} \end{bmatrix} = g_{00}^{(n)} \begin{bmatrix} 1 & f^{(n)} \\ f^{(n)} & 1 \end{bmatrix} \begin{bmatrix} j_0^{(n)} \\ j_1^{(n)} \end{bmatrix}.$$

It can be shown that $f^{(n)}=f_1^{(n)}(f_2^{(n)}(s))$, where $f_1^{(n)}$ and $f_2^{(n)}$ are the first passage time functions for the fractals $\mathcal{F}(1)$ and $\mathcal{F}(2)$ that occur in the nth generation. An example of this relationship is given in Appendix B. Careful examination of the first passage time shows that the functional relationship satisfied by $f^{(n)}$ and $f^{(n+1)}$ for the composite fractal is exactly

$$f^{(n)}\{(f_2^{(n)})^{-1}[\rho_1(f_2^{(n)}(\rho_2(s)))]\} = f^{(n+1)}(s).$$

The combination of functions appearing in the argument of the left-hand side depends on n and therefore no ρ^* exists that can relate all $f^{(n)}$ to $f^{(n+1)}$ as in prior sections. However, an analogous result can be shown for small s, which is all that is needed to calculate the spectral dimension.

The expansion of the first passage time of the fractal $\mathcal{F}(2)$ is $f_2^{(0)}=1-\gamma_2 s+O(s^2)$ because the underlying first passage time is a probability density (so $f_2^{(0)}|_{s=0}=1$). Using Eq. (14) and the expansion $\rho(s)=a_2^{v(2)}s+O(s^2)$ implies that

$$f_2^{(n)}(s) = f_2^{(0)}(\rho(\rho(\cdots))) = 1 - \gamma_2 a_2^{nv(2)} s + O(s^2).$$

Similarly $f_1^{(n)}=1-\gamma_1 a_1^{v(1)n}s$ for the fractal $\mathcal{F}(1)$. Combining these results gives

$$(f_2^{(n)})^{-1}[\rho_1(f_2^{(n)}(\rho_2(s)))] = \frac{a_1^{v(1)}\gamma_2 a_2^{v(2)n} a_2^{v(2)}}{\gamma_2 a_2^{v(2)n}} s + O(s^2) = a_1^{v(1)} a_2^{v(2)} s + O(s^2).$$

If we define $\rho^*(s)=\rho_1(\rho_2(s))$, which has a Taylor series expansion of $\rho^*(s)=a_1^{v(1)}a_2^{v(2)}s+O(s^2)$, then $f^{(n)}(\rho^*(s)) = f^{(n+1)}(s)+O(s^2)$.

Now consider the Green's function $g_{00}^{(n)}$ for ℓ_n. We know that as $s\to 0$, $g_{00}^{(n)}=1/(A_n s)+O(s^0)$ and therefore $g_{00}^{(n)}/g_{00}^{(n+1)} = A_{n+1}/A_n+O(s)=A+O(s)$, where A is the increase in mass from ℓ_n to ℓ_{n+1}. Now since

$$\frac{g_{00}^{(n+1)}(\rho^*(s))}{g_{00}^{(n)}(\rho^*(s))} = \frac{g_{00}^{(n+2)}(s)}{g_{00}^{(n+1)}(s)} + O(s),$$

our key equation

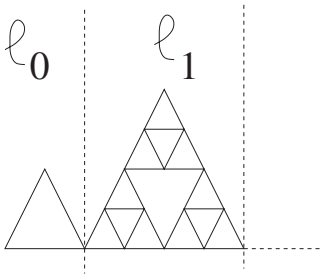

FIG. 7. A Sierpinski gasket tree, with $v(1)=2$, $v(2)=-1$, $u=1$.

$$c_0 = g_{00}^{(0)} - (g_{01}^{(0)})^2\left(g_{00}^{(0)} + \frac{\xi^{(1)}c_0(\rho^*)}{u\xi^{(0)}(\rho^*)}\right)^{-1}$$

holds up to leading order. This is the only requisite needed to calculate the spectral dimension

$$\bar{d} = \frac{v(1)\bar{d}_{\mathcal{F}(1)}\ln(a_1) + v(2)\bar{d}_{\mathcal{F}(2)}\ln(a_2) + 2\ln(u)}{v(1)\ln(a_1) + v(2)\ln(a_2)}. \quad (28)$$

Note that we do not require all $v(i)>0$ in the above formulation. This is demonstrated on a network composed of two fractals; the Sierpinski gasket and the 1D bar, shown in Fig. 7. We have taken ℓ_n to be the $(2n)$th iteration of the Sierpinski gasket $[\mathcal{F}(1)]$ and $\mathcal{F}(2)$ to be a shrinking pipe of length 2^{-n}. Equation (28) gives $\bar{d}=2\ln(9/2)/\ln(25/4)$. We have computationally checked this value on a network with $n=13$, implying that the final subnetwork is the 26th iteration of the Sierpinski gasket made from pipes of length 2^{-13}. The Laplace transform was inverted using the algorithm of Abate and Witt [35] and is shown in Fig. 8. Note the oscillations in the exact result are expected and have been the focus of various studies [36,37].

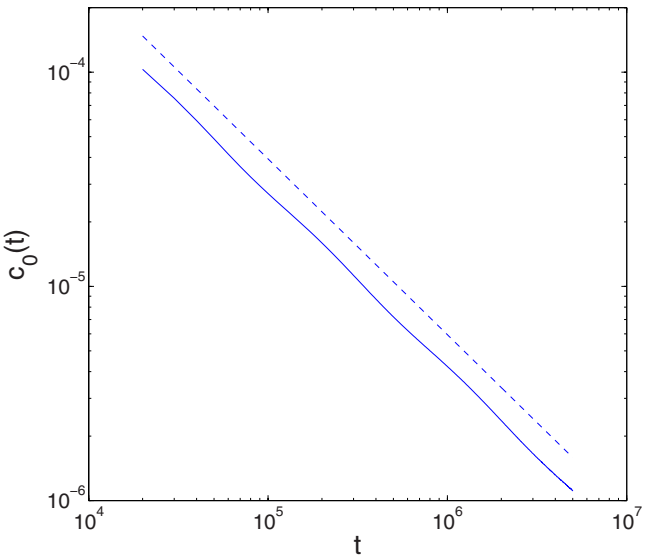

FIG. 8. (Color online) A log-log plot of c_0 for the Sierpinski gasket tree shown in Fig. 7. The solid line shows the numerical calculation and the dashed line gives the analytic result. The analytic result has been vertically shifted for comparison.

The above method can be extended to multiple fractals. With the obvious extension of notation, the spectral dimension for M fractals is

$$\bar{d} = 2\frac{\ln(Au)}{\ln\left(\prod_{i=1}^{M} a_i^{v(i)}\right)} \quad \text{and} \quad A = \prod_{i=1}^{M} a_i^{v(i)\bar{d}_{\mathcal{F}(i)}/2}.$$

VIII. SUBNETWORKS

The reason that we were able to find $\bar{d}$ in prior sections is because the first passage times and the Green's function g_{00} satisfied the renormalization equations (14) and (15). In this section we show how these equations can be used for general subnetworks (i.e., not necessarily fractal). First we examine the case where the basic pipe of the Bethe lattice (see Fig. 1) is replaced by an arbitrary finite subnetwork ℓ_0, with two end nodes denoted by 0 and 1. We define ℓ_1 to be identical to ℓ_0 except that the internal pipes are replaced by pipes of length 2^v [see Fig. 2(d)], i.e., ℓ_1 is a scaled up version of ℓ_0.

Consider the flux-concentration matrix for a pipe in the subnetwork ℓ_n written in the form

$$\xi_p^{(n)}[1-(f_p^{(n)})^2]\begin{bmatrix} j_0^{(n)} \\ j_1^{(n)} \end{bmatrix} = \begin{bmatrix} 1 & -f_p^{(n)} \\ -f_p^{(n)} & 1 \end{bmatrix}\begin{bmatrix} c_n \\ c_{n+1} \end{bmatrix}.$$

Here $\xi_p^{(n)}$ and $f_p^{(n)}$ are the return to origin and first passage time functions for a pipe of length 2^{vn}. We use this notation to differentiate between the Green's function of the pipe ξ_p and of the subnetwork, which is denoted by g_{00} as in earlier sections.

For an arbitrary subnetwork of N nodes, the flux-concentration equations of ℓ_n will have the form

$$\xi_p^{(n)}[1-(f_p^{(n)})^2]\mathbf{j} = E(f_p^{(n)})\mathbf{c},$$

where E is an $N\times N$ matrix. All entries of E are either constants or multiples of $f_p^{(n)}$ (for example, see Appendix B).

We now calculate the flux-concentration matrix $\bar{E}$ for the effective reduced network by eliminating $N-2$ equations (as shown in the previous section and Appendix B) to give $\xi_p^{(n)}[1-(f_p^{(n)})^2]\mathbf{j}=\bar{E}(f_p^{(n)})\mathbf{c}$. Inverting the 2×2 matrix $\bar{E}(f_p^{(n)})$ gives $\xi_p^{(n)}Q(f^{(n)})\mathbf{j}=\mathbf{c}$, where $Q(f_p^{(n)})=[1-(f_p^{(n)})^2]\bar{E}^{-1}(f_p^{(n)})$. The elements of Q, $q_{ij}^{(n)}(s)$, depend only on the first passage time $f_p^{(n)}$ of the pipe. Since $f_p^{(n)}(\rho(s))=f_p^{(n+1)}(s)$ and E (and therefore $\bar{E}$) are independent of n it follows that $q_{ij}^{(n)}(\rho(s))=q_{ij}^{(n+1)}(s)$. Given that q_{ij} has this property, we can repeat the renormalization procedure demonstrated in Sec. IV.

First, the equivalent infinite continued fraction for the network composed of subnetworks $\ell_0,\ell_1,\ldots$, is found by taking $j_0^{(n)}=h_n c_n$ and $j_1^{(n)}=-uh_{n+1}c_{n+1}$ in

$$\xi_p^{(n)}\begin{bmatrix} q_{00}^{(n)} & q_{01}^{(n)} \\ q_{10}^{(n)} & q_{11}^{(n)} \end{bmatrix}\begin{bmatrix} j_0^{(n)} \\ j_1^{(n)} \end{bmatrix} = \begin{bmatrix} c_n \\ c_{n+1} \end{bmatrix},$$

to get

$$(\xi_p^{(n)}h_n)^{-1} = q_{00}^{(n)} - q_{01}^{(n)}[q_{11}^{(n)} + (\xi_p^{(n)}uh_{n+1})^{-1}]^{-1}q_{10}^{(n)}.$$

This is the counterpart to Eq. (8) and can be renormalized since

$$q_{ij}^{(0)}(\rho(s)) = q_{ij}^{(1)}(s) \quad \text{and} \quad \frac{\xi_p^{(n+1)}(\rho(s))}{\xi_p^{(n)}(\rho(s))} = \frac{\xi_p^{(n+2)}(s)}{\xi_p^{(n+1)}(s)}.$$

The second equation holds because $\xi_p^{(n+1)}$ is the return to origin Green's function of a single pipe. Hence a similar form to Eq. (16) can be derived,

$$[\xi_p^{(n)}(\rho)h_n(\rho)]^{-1} = (\xi_p^{(n+1)}h_{n+1})^{-1},$$

giving

$$c_0 = g_{00}^{(0)} - g_{01}^{(0)}\left(g_{11}^{(0)} + \frac{\xi_p^{(1)}c_0(\rho)}{u\xi_p^{(0)}(\rho)}\right)^{-1} g_{10}^{(0)}.$$

Series expansions of the above reveal that the spectral dimension of the network is still given by Eq. (22) so the introduction of the subnetwork does not alter $\bar{d}$. We have included the results for completeness, and note that they are important for handling more general networks [38]. Of course the basic pipes of the finite subnetwork can be replaced by fractals as in prior sections.

IX. CONCLUSION

We have calculated the spectral dimension for several classes of homogeneous and inhomogeneous networks through the renormalization of a continued fraction. These results expand the number of model structures with analytically known spectral dimensions. It was possible to derive the results for the fractal and composite fractal networks because of the interesting first passage renormalization function $\rho(s)$ [33,34]. In this paper we have shown how to exploit this function in a general formulation of diffusion on networks. Importantly, we were able to prove that certain ratios of Green's functions could be renormalized using $\rho(s)$, allowing us to find a functional relationship between $c_0(s)$ and $c_0(\rho(s))$ for quite general structures.

The inhomogeneous trees considered in Sec. V appear to be new and may prove useful for modeling hyperbranched polymers [17]. It is interesting that the spectral dimension of the inhomogeneous trees have the same form as that obtained for bundled structures [13] even though they can be structurally quite different. In the final section we generalized the renormalization scheme to any finite subnetwork. Even though the growing subnetworks may contain loops of increasing size, the fact that $\bar{d}$ is not altered, indicates that there is insufficient coupling between the loops at different scales to fundamentally change diffusive transport.

An unusual aspect of this paper is that all of the analysis has been performed for a continuum random walker. This may prove directly useful for certain physical problems [19,20] which are more naturally formulated in the continuum. In addition, we believe that the analysis of diffusion on networks is simpler using the continuum formulation. In particular, the coordination number at each node, which fea-

tures strongly in analyses for discrete walkers does not appear. As a consequence, the flux-concentration matrix is symmetric and the series expansions of the Green's functions are simpler. As we have established a direct correspondence between continuum and discrete walkers in an earlier paper [21], the continuum formulation may prove useful in future studies of discrete random walkers.

It is interesting that the continued fraction framework is able to provide an analytic route into so many different problems. Although we have only used this framework for structures with two end nodes, in future work [38] we show how it can be generalized to investigate branching trees made from interconnected branches with two or more starting nodes and two or more end nodes.

APPENDIX A: PROBABILISTIC INTERPRETATION

In this appendix we demonstrate the probabilistic interpretation of the elements of the matrices which arise in the flux-concentration equations. Solving the flux-concentration equations (2) of the pipe with $j_0=1$ and $j_1=0$ gives $\mathbf{c}^T=(g_{00},g_{10})$. g_{00} is the Laplace transform of the probability that a walker released at site 0 at $t=0$ is at site 0 at later times on the closed pipe (i.e., it is a Green's function). Similarly g_{10} is the Laplace transform of the probability that a walker released at site 0 at $t=0$ is at site 1 at subsequent times. Setting $\mathbf{j}^T=(0,1)$ gives g_{01} and g_{11}. We can write the combination of both problems as $\mu I=EG$, where the elements of G are g_{ij}.

The relationship with first passage times is found by rewriting Eq. (2) in terms of Green's functions and considering the problem

$$\begin{bmatrix} g_{00} & g_{01} \\ g_{10} & g_{11} \end{bmatrix}\begin{bmatrix} j_0 \\ 1 \end{bmatrix}=\begin{bmatrix} 0 \\ c_1 \end{bmatrix}.$$

If we solve this system, j_0 represents the Laplace transform of the flux at site 0 given that a source is released at site 1 at $t=0$. The first equation shows that $j_0=-g_{01}/g_{00}$. It is negative because j_0 is the flux entering at site 1. By definition, the flux into a trap is identical to the first passage time density function f. Similarly $-j_1=g_{10}/g_{11}$. The results are convolutions in time and can also be derived using random walker arguments [26].

APPENDIX B: DETERMINISTIC TREE

In this appendix we provide sample calculations for the deterministic tree which illustrate key ideas in the paper. The flux-concentration equations for the deterministic tree shown in Fig. 9(b) are $\mu\mathbf{j}=E(\sigma_0)\mathbf{c}$, where

$$E(\sigma_0)=\begin{bmatrix} 1 & 0 & -\sigma_0 & 0 & 0 \\ 0 & 1 & -\sigma_0 & 0 & 0 \\ -\sigma_0 & -\sigma_0 & 4 & -\sigma_0 & -\sigma_0 \\ 0 & 0 & -\sigma_0 & 1 & 0 \\ 0 & 0 & -\sigma_0 & 0 & 1 \end{bmatrix} \tag{B1}$$

and $\sigma_0=\mathrm{sech}(\sqrt{s})$. To find the effective reduced network between nodes 0 and 1, we set $j_2=j_3=j_4=0$. The concentrations

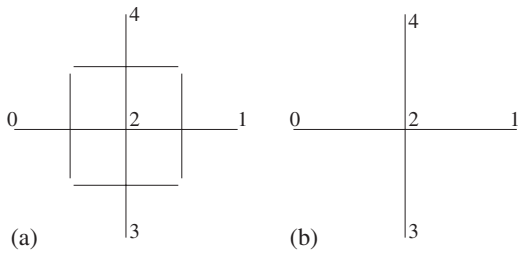

FIG. 9. (a) First iteration of a deterministic tree. (b) Zeroth iteration of the tree. The node labeling is used in Appendix B.

at the nodes 2, 3, and 4 can be expressed in terms of c_0 and c_1 as

$$\begin{bmatrix} c_2 \\ c_3 \\ c_4 \end{bmatrix}=1/2\frac{\sigma_0}{2-\sigma_0^2}\begin{bmatrix} 1 & 1 \\ \sigma_0 & \sigma_0 \\ \sigma_0 & \sigma_0 \end{bmatrix}\begin{bmatrix} c_0 \\ c_1 \end{bmatrix}.$$

Using these equations in Eq. (B1) gives

$$\mu\begin{bmatrix} j_0 \\ j_1 \end{bmatrix}=1/2\frac{4-3\sigma_0^2}{2-\sigma_0^2}\begin{bmatrix} 1 & \frac{-\sigma_0^2}{4-3\sigma_0^2} \\ \frac{-\sigma_0^2}{4-3\sigma_0^2} & 1 \end{bmatrix}\begin{bmatrix} c_0 \\ c_1 \end{bmatrix}. \tag{B2}$$

These are the equations for the effective reduced network between nodes 0 and 1 of the tree. The above equations can be rewritten as

$$g_{00}(1-\sigma_1^2)\mathbf{j}=\begin{bmatrix} 1 & -\sigma_1 \\ -\sigma_1 & 1 \end{bmatrix}\begin{bmatrix} c_0 \\ c_1 \end{bmatrix}, \tag{B3}$$

where $g_{00}=(4-3\sigma_0^2)\mu/[4(1-\sigma_0^2)]$ and $\sigma_1=\frac{\sigma_0^2}{4-3\sigma_0^2}$ is the first passage time of the reduced sub-network.

The next iteration of the tree is constructed from four copies of the zeroth iteration [see Fig. 9(a)]. The full 17×17 flux-concentration matrix for $n=1$ can be replaced by a 5×5 matrix with the elements taken from the matrix of the effective reduced network equations (B2) or (B3) for the zeroth iteration. This gives

$$\mu\mathbf{j}=1/2\frac{4-3\sigma_0^2}{2-\sigma_0^2}E(\sigma_1)\mathbf{c}, \tag{B4}$$

where $E(\sigma_1)$ is the matrix $E(\sigma_0)$ shown in Eq. (B1) with σ_0 replaced by σ_1. For the next iteration we have

$$\mu\mathbf{j}=1/4\frac{4-3\sigma_1^2}{2-\sigma_1^2}\frac{4-3\sigma_0^2}{2-\sigma_0^2}E(\sigma_2)\mathbf{c}. \tag{B5}$$

This process can obviously be extended. Note that the renormalization procedure implies that $\sigma_n(s)=\sigma_{n-1}(\hat{\rho}(s))=\sigma_{n-2}(\hat{\rho}(\hat{\rho}(s)))=\cdots$ for some $\hat{\rho}(s)$. For the deterministic tree $\hat{\rho}(s)=\mathrm{arcsech}[\sigma_0^2/(4-3\sigma_0^2)]^2$. As mentioned in the text the pipe can be interpreted as a fractal, in which case $\hat{\rho}(s)=4s$. In Sec. VI, we allow for the fractals in generation n of the network to be of iteration vn (v integer). From the above it is clear that $\rho(s)=\hat{\rho}(\hat{\rho}(\cdots))v$ times where $\hat{\rho}$ is the corresponding

function for $\upsilon=1$. If $\hat{\rho}=as+O(s^2)$ then $\rho=a^{\upsilon}s+O(s^2)$. These expansions are required throughout the text.

In Sec. VII we consider fractal subnetworks where the pipes are constructed from a different fractal. The above example can be extended to this case as follows. Suppose we replace each pipe of the zeroth iteration of the deterministic tree by the zeroth iteration of the Sierpinski gasket. Equation (B3) for the gasket is

$$g_{00}^{\star}(1-\tau_1^2)\mathbf{j}=\begin{bmatrix}1 & -\tau_1\\ -\tau_1 & 1\end{bmatrix}\mathbf{c},$$

where $\tau_1=\tau_0/(2-\tau_0)$, $\tau_0=\sigma_0=\mathrm{sech}(\sqrt{s})$, and $g_{00}^{\star}=(\tau_0-2)\mu/[2(\tau_0-1)(2+\tau_0)]$. Now for the composite network equation, Eq. (B3) is replaced by

$$g_{00}^{\star\star}[1-\sigma_1(\tau_1)^2]\mathbf{j}=\begin{bmatrix}1 & -\sigma_1(\tau_1)\\ -\sigma_1(\tau_1) & 1\end{bmatrix}\mathbf{c},$$

where $g_{00}^{\star\star}=g_{00}^{\star}(4-3\tau_1^2)/4$. The first passage time of the zeroth iteration of the composite lattice is therefore $f^{(0)}(s)=\sigma_1(\tau_1(s))$.

APPENDIX C: RATIO OF GREEN'S FUNCTIONS

In this section, we show that the Green's function $g_{00}^{(n)}$ for any finitely ramified deterministic symmetric fractal has the property (15) required for the renormalization argument.

For the zeroth iteration of a fractal, the flux concentration equations are $\mu\mathbf{j}=E(\sigma_0)\mathbf{c}$, where $E_0(\sigma_0)$ is a matrix with depends only on σ_0 [e.g., Eq. (B1)]. For the next iteration, the full flux-concentration equations can be reduced to the form of the zeroth iteration by employing reduced networks. The resultant equations can be written as

$$\mu\mathbf{j}=\gamma(\sigma_0)E(\sigma_1)\mathbf{c},$$

where $\gamma(\sigma_0)$ is a known function [see, e.g., Eq. (B4)]. In Appendix B, we showed that $\sigma_n=\sigma_{n-1}^2/(4-3\sigma_{n-1}^2)$ for the deterministic tree. In general the form of σ_n depends on the type of fractal. Repeating the procedure for higher iterations, the flux concentration equations can be expressed in the form [e.g., Eq. (B5)]

$$\mu\mathbf{j}=\left(\prod_{i=0}^{n-1}\gamma(\sigma_i)\right)E(\sigma_n)\mathbf{c}. \tag{C1}$$

Now g_{00} is the first element of the Green's function matrix,

$$g_{00}^{(n)}=\mu[E^{-1}(\sigma_n)]_{00}\prod_{i=0}^{n-1}\frac{1}{\gamma(\sigma_i)},$$

where $[E^{-1}(\sigma_n)]_{00}$ is the first element of E^{-1}. The key quotient can be written as

$$\frac{g_{00}^{(n+1)}}{g_{00}^{(n)}}=\frac{[E^{-1}(\sigma_{n+1})]_{00}}{[E^{-1}(\sigma_n)]_{00}}\frac{1}{\gamma(\sigma_{n+1})},$$

and furthermore using $\sigma_n(s)=\sigma_{n-1}(\rho(s))$ we have

$$\frac{g_{00}^{(n+1)}(\rho(s))}{g_{00}^{(n)}(\rho(s))}=\frac{[E^{-1}(\sigma_{n+2})]_{00}}{[E^{-1}(\sigma_{n+1})]_{00}}\frac{1}{\gamma(\sigma_{n+2})}=\frac{g_{00}^{(n+2)}(s)}{g_{00}^{(n+1)}(s)}.$$

Note that although the above proof has been given for $\upsilon=1$, it can be extended for any $\upsilon\geqslant 2$.

[1] D. Cassi, Phys. Rev. Lett. **68**, 3631 (1992).
[2] P. Argyrakis and R. Kopelman, Chem. Phys. **261**, 391 (2000).
[3] E. W. Montroll, J. Math. Phys. **10**, 753 (1969).
[4] S. Alexander and R. Orbach, J. Phys. (Paris), Lett. **19**, L625 (1982).
[5] B. O'Shaughnessy and I. Procaccia, Phys. Rev. A **32**, 3073 (1985).
[6] S. Havlin and D. ben Avraham, Adv. Phys. **51**, 187 (2002).
[7] R. Burioni and D. Cassi, J. Phys. A **38**, R45 (2005).
[8] B. B. Mandelbrot, *The Fractal Geometry of Nature* (Freeman, San Francisco, 1982).
[9] D. Cassi, Int. J. Mod. Phys. B **6**, 85 (1992).
[10] A. Franz, C. Schulzky, S. Seeger, and K. H. Hoffmann, Fractals **8**, 155 (2000).
[11] H. D. Rozenfeld, S. Havlin, and D. ben Avraham, New J. Phys. **9**, 175 (2007).
[12] D. Cassi and S. Regina, Phys. Rev. Lett. **70**, 1647 (1993).
[13] D. Cassi and S. Regina, Phys. Rev. Lett. **76**, 2914 (1996).
[14] R. Burioni, D. Cassi, A. Pirati, and S. Regina, J. Phys. A **31**, 5013 (1998).
[15] R. Burioni and D. Cassi, Phys. Rev. E **51**, 2865 (1995).
[16] H. L. Martinez, J. M. R. Parrondo, and K. Lindenberg, Phys. Rev. E **48**, 3545 (1993).
[17] A. Blumen, A. Jurjiu, Th. Koslowski, and Ch. von Ferber, Phys. Rev. E **67**, 061103 (2003).
[18] D. S. Grebenkov, M. Filoche, B. Sapoval, and M. Felici, Phys. Rev. Lett. **94**, 050602 (2005).
[19] V. E. Arkhincheev, Physica A **307**, 131 (2002).
[20] J. Koplik, S. Redner, and D. Wilkinson, Phys. Rev. A **37**, 2619 (1988).
[21] C. P. Haynes and A. P. Roberts, Phys. Rev. E **78**, 041111 (2008).
[22] W. Woess, *Random Walks on Infinite Graphs and Groups* (Cambridge University Press, Cambridge, England, 2000).
[23] B. D. Hughes and M. Sahimi, J. Stat. Phys. **29**, 781 (1982).
[24] D. Cassi, Europhys. Lett. **9**, 627 (1989).
[25] D. Cassi and S. Regina, Mod. Phys. Lett. B **9**, 601 (1995).
[26] B. D. Hughes, *Random Walks and Random Environments* (Clarendon Press, Oxford, 1996), Vol. 1.
[27] M. Abramowitz and I. A. Stegun, *Handbook of Mathematical Functions* (Dover, New York, 1972).
[28] D. Cassi and S. Regina, Mod. Phys. Lett. B **6**, 1397 (1992).
[29] R. E. Grundy, J. Inst. Math. Appl. **20**, 299 (1977).
[30] D. V. Widder, *The Laplace Transform* (Princeton University Press, Princeton, 1941).

[31] R. Burioni and D. Cassi, Phys. Rev. E **49**, R1785 (1994).
[32] K. Hattori, T. Hattori, and H. Watanabe, Prog. Theor. Phys. **92**, 108 (1987).
[33] C. Van den Broeck, Phys. Rev. A **40**, 7334 (1989).
[34] C. Van den Broeck, Phys. Rev. Lett. **62**, 1421 (1989).
[35] J. Abate and W. Whitt, ORSA J. Comput. **7**, 36 (1995).
[36] J. Klafter, G. Zumofen, and A. Blumen, J. Phys. A **24**, 4835 (1991).
[37] E. Teufl, Combinatorics, Probab. Comput. **12**, 203 (2003).
[38] C. P. Haynes and A. P. Roberts (unpublished).